

Original scientific paper

**PERFORMANCE EVALUATION OF A MULTICARRIER
MIMO SYSTEM BASED ON DFT-PRECODING
AND SUBCARRIER MAPPING**

**Fahad Bin Muslim¹, Muntazir Hussain², Usman Hashmi¹, Aneesullah³,
Muhammad Aamir⁴, Ali Zahir⁵**

¹Department of Computing and Technology, Iqra University, Islamabad, Pakistan

²Department of Electrical and Computer Engineering, Air University, Islamabad, Pakistan

³Department of Electronics Engineering, University of Engineering and Technology
Peshawar, Pakistan

⁴Department of Electrical and Computer Engineering, Pak Austria Fachhochschule
Institute of Applied Science and Technology, Haripur, Pakistan

⁵Department of Electrical and Computer Engineering, Comsats University Islamabad,
Abbottabad, Pakistan

Abstract. *The ever-increasing end user demands are instigating the development of innovative methods targeting not only data rate enhancement but additionally better service quality in each subsequent wireless communication standard. This quest to achieve higher data rates has compelled the next generation communication technologies to use multicarrier systems e.g. orthogonal frequency division multiplexing (OFDM), while also relying on the multiple-input multiple-output (MIMO) technology. This paper is focused on implementing a MIMO-OFDM system and on using various techniques to optimize it in terms of the bit-error rate performance. The test case considered is a system implementation constituting the enabling technologies for 4G and beyond communication systems. The bit-error rate optimizations considered are based on preceding the OFDM modulation step by Discrete Fourier Transform (DFT) while also considering various subcarrier mapping schemes. MATLAB-based simulation of a 2×2 MIMO-OFDM system exhibits a maximum of 2 to 5 orders of magnitude reduction in bit-error rate due to DFT-precoding and subcarrier mapping respectively at high signal-to-noise ratio values in various environments. A 2-3dBs reduction in peak-to-average power ratio due to DFT-precoding in different environments is also exhibited in the various simulations.*

Key words: *MIMO-OFDM, Bit-error rate, Multiple access, Diversity, Amplifier nonlinearities.*

Received September 9, 2021; received in revised form December 23, 2021

Corresponding author: Fahad Bin Muslim

Department of Computing and Technology, Iqra University, Islamabad, Pakistan

E-mail: fahad@iqraisb.edu.pk

1. INTRODUCTION

The concept of multicarrier modulation has revolutionized the modern communication technologies quite profoundly. While orthogonal frequency division multiplexing (OFDM) has been around since long and had been a part of the radio access technologies till 4G, other modified techniques such as non-orthogonal multiple access (NOMA) and filtered OFDM (F-OFDM) are being seen as the waveforms of choice for 5G and beyond [1-3]. OFDM causes great enhancement in spectral efficiency besides providing performance boost in environments consisting of high frequency selectivity. Moreover, the equalization process is also greatly simplified by OFDM owing to each of the subcarrier experiencing flat fading. This essentially implies the application of a single tap equalizer which represents a simple delay operation wherein, the equalization is accomplished by using a previously detected symbol [4].

Furthermore, the key towards delivering upon the promises made in performance by modern communication standards, is the use of multi-antenna arrays i.e. multiple-input multiple-output (MIMO) systems. These networks utilize MIMO to create several physical routes from the transmitter to the receiver in order to deliver greater streams of data within the same time and frequency blocks. Some of the key features of MIMO systems responsible for delivering an enhanced capacity and spectral efficiency as expected from 5G networks, are the spatial diversity and spatial multiplexing [5]. In the former, the same signal is transmitted over several different paths, each experiencing an independent channel realization while the later comprises of different signals sent over different paths. These features of MIMO lead to an improved data rate as well as an increased signal-to-noise ratio (SNR) owing to the so-called diversity combining [6]. The two features are depicted in the Fig. 1 where the blue dotted lines depict the spatial diversity while the spatial multiplexing is shown by the red and green dotted lines. MIMO is already being used in 4G while its scaled version consisting of a considerably larger array of antennas (in 100s), the so-called massive MIMO, is a strong contender to be used in 5G [7]. Owing to the requirement of having a reliable high-speed wireless communication, OFDM in combination with MIMO technology is an attractive combination for upcoming generations of wireless communications. This ensures the best of both the worlds i.e. the energy and spectral efficiency of MIMO combined with the spectral efficiency and the ease in equalization offered by OFDM [5, 8]. The main theme of this paper is hence, based on the implementation and analysis of a MIMO-OFDM system.

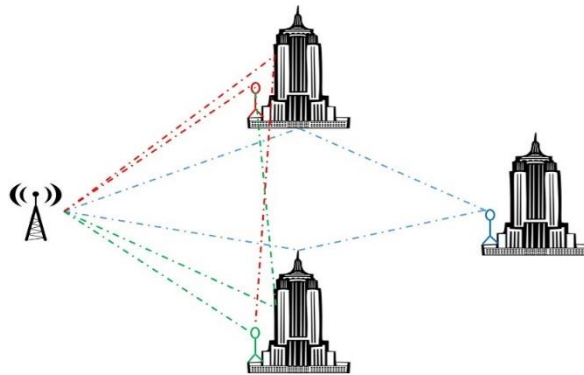


Fig. 1 Spatial diversity and multiplexing in MIMO

The main contribution of this work is to implement a MIMO-OFDM system and its multiaccess version considering both the linear environment and the nonlinear environment. The system is then analyzed in terms of the bit-error rate (BER) performance considering Discrete Fourier Transform-precoding (DFT-precoding). This is followed by using various subcarrier mapping schemes and analyzing their impact on the BER. The underlying aspect of peak-to-average power ratio (PAPR) variation plays an important role in the BER performance variation especially in nonlinear environments. Hence, the PAPR analysis of the various test cases is also being performed. The two techniques are not used primarily for BER improvement while a similar analysis on a MIMO-OFDM system has not been found in the literature (see section 3) to the best knowledge of the authors. This hence, motivated us to align our work in this direction.

The rest of the paper is structured as follows. The background on DFT-precoding and subcarrier mapping is provided in section 2. Some relevant work found in literature is presented in section 3. Section 4 is dedicated to some discussion on the system model. The simulation results, in terms of the BER performance and the PAPR, are presented in section 5. Finally, the work is concluded in section 6.

2. DFT-PRECODING AND SUBCARRIER MAPPING

The issue with the systems employing OFDM is the poor power efficiency owing to its excessive PAPR. This high PAPR results in inefficiency while using high-power amplifier (HPA) on the transmitter side of International Mobile Telecommunication-Advanced (IMT-Advanced) [9] since it enters the nonlinear region of operation. The operating efficiency in HPA can be maximized if it is operated in the saturation region of operation. Low PAPR ensures that the HPA operates near the linear region. Besides, low PAPR is critical especially in the uplink since, the user equipment (UE) has a limited source of energy i.e. its battery [10].

2.1. DFT-precoding

Various techniques can be used to keep the OFDM peak-to-average power ratio within reasonable limits. One such technique is DFT-precoding being employed e.g. in uplink in several wireless communication standards including Long term evolution (LTE) and its successor, the LTE-advanced. Among several alternatives, DFT-precoding presents a favorable choice as it can be implemented by merely using the Fast Fourier Transform (FFT) prior to OFDM modulation and it does not require any extra signal overhead. OFDM preceded by DFT-precoding causes a reduction in envelope variations in comparison to the conventional OFDM system. This reduction is because of the sharing of the subcarrier bandwidth among the whole of the subcarriers in a DFT-precoded OFDM. The conventional OFDM in comparison, encompasses the superposition of all the subcarriers over the signal bandwidth.

Owing to the spreading effect experienced by every data symbol over several subcarriers in an OFDM system precoded by DFT, this technique is also sometimes termed as a single-carrier frequency division multiplexing (SC-FDM). This results in spreading gain in a SC-FDM system [11]. Because of the spreading gain inherent to DFT-precoded OFDM, it is also sometimes termed as DFT-spread OFDM.

2.2. Subcarrier mapping

Subcarrier (SC) mapping following the DFT-precoding converts an OFDM system into its multiaccess counterpart i.e. the orthogonal frequency division multiple access (OFDMA) [12]. This mapping results in any N DFT-precoded symbols being spread among a combination of any M subcarriers such that M is greater than N . The subcarriers may be mapped in a localized fashion termed localized FDMA (LFDMA) or in a distributed fashion termed distributed FDMA (DFDMA). The former comprises of assigning consecutive subcarriers to the users while in the latter, an offset is introduced between subcarriers being assigned to each user. Among the two schemes however, DFDMA offers more diversity owing to greater spreading of the subcarriers, as compared to LFDMA. The trade-off, on the other hand, is the increased pilot overhead in DFDMA needed for channel estimation as compared to LFDMA [11, 13].

Another scheme that is a compromise between the two is the block-interleaved FDMA (BIFDMA). This scheme consists of equidistant group/chunk of greater than one subcarrier being assigned to each user. Grouping of subcarriers (instead of using individual subcarriers as in DFDMA) gives this scheme a flavor of the LFDMA while interleaving between the groups gives it a flavor of DFDMA [14]. The three subcarrier mapping schemes are illustrated in Fig. 2.

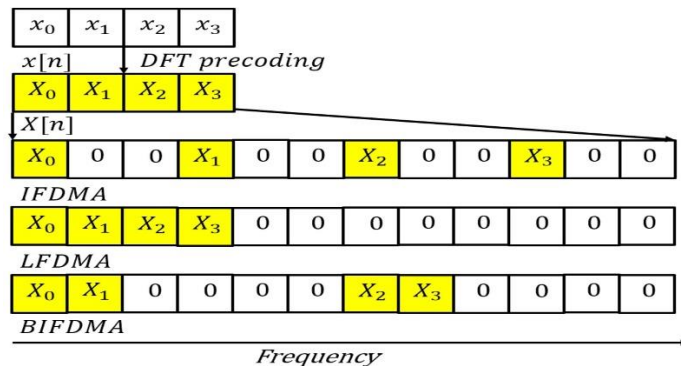


Fig. 2 Comparison of IFDMA, LFDMA and BIFDMA

3. RELATED WORK

The concept of MIMO and its affiliated advantages has been under active research since long. At the same time, the added advantage that OFDM can offer in a MIMO communication system had also been acknowledged long ago in the research community. Various aspects of MIMO-OFDM have thereafter, remained areas of active research including the BER performance analysis of such systems. In this section, we present some relevant work done in this regard.

In this context, several papers e.g. [15], compared the BER performance of a simple OFDM system with a MIMO-OFDM system. The analysis in this paper has been made under AWGN, Rayleigh and Rician fading environments by considering convolutional coding. The system implementation in this work has been carried out by considering a software-defined radio (SDR) platform like the one considered in [5]. The paper, however, only considers the

differences in performance between a simple OFDM and MIMO-OFDM systems communicating over various channels and including the impact of repetition coding.

A research similar to [15] has been done in [16] to compare the BER performance of various MIMO antenna configurations while considering the same channels as considered in [15] and various digital modulation formats i.e. BPSK, QPSK, 16QAM and 64QAM. The work also includes implementing several error-correction codes. The authors have considered binary and image data and have tried to select the best options among the considered configurations in terms of BER performance. A hardware field programmable gate array (FPGA) based implementation of a 2×2 MIMO-OFDM system considering rateless space-time block code (RSTBC) has been performed in [17] and the results compared with simulations to verify the correctness of the hardware implementation. All the works considered so far i.e. [15-17] however, do not consider the aspects of PAPR reduction, nonlinearities and multiaccess that have been discussed in this work.

A DFT spread MIMO-OFDM system is considered in [18]. The author has proposed a frequency domain representation of Tomlinson-Harashima precoding (THP) for MIMO-OFDM in this work and performed BER analysis of his proposed algorithms with generic minimum mean square error (MMSE) decoder. Similarly, DFT-precoded MIMO-OFDM systems have been considered in [19] and [20] for underwater acoustic communication. The main consideration in both these papers, however, has been to research the use of this technique widely used in wireless communication, in underwater communications. This makes the focus in those works considerably different than what we are trying to achieve here. Additionally, a MIMO-OFDMA system is considered in [21] wherein, the authors propose a quarter ICI self-cancellation (ICI-SC) subcarrier scheme to overcome the inter-carrier interference caused by frequency offset inherent to OFDMA systems. The authors, however, do not consider the DFT-precoding and similarly the SC mapping schemes considered in this work are also non-existent.

A PAPR reduction technique in a MIMO-OFDM system has recently been proposed in [22] wherein, a hybrid approach combining turbo coding and enhanced switching differential algorithm-based partial transmit sequence is considered to accomplish PAPR as well as BER reduction. The authors of [22] also propose another approach in [23] for massive MIMO-OFDM systems by incorporating a distributive population-based switching differential evolution strategy in the selected matching technique that also achieves significant PAPR reduction. In both the cases, the specific methodology to accomplish reduction in PAPR (and BER) is however, considerably different as compared to what we are accomplishing in this study. Thus, PAPR reduction in systems based on MIMO-OFDM and the resulting BER improvement is actively being pursued in the research community and is therefore the main theme of this research study as well.

4. SYSTEM MODEL

In this section, we explain the basic system model that has been implemented. A 2×2 MIMO channel is considered with two transmit and two receive antennas. A simple zero forcing (ZF) equalization is considered in this work which reduces the channel experienced by every symbol being transmitted from each antenna to a simple 1×1 Rayleigh fading channel [24]. The implemented system model based on [25] in the form of a block diagram is depicted in Fig. 3. Some assumptions are being made while implementing the system model. It is assumed that

the various transmitted signal streams encounter independent channel realizations. Moreover, it is also assumed that each signal travelling from a transmit antenna to a receive antenna is multiplied by a random Rayleigh channel coefficient and is corrupted by a gaussian distributed noise with mean 0. The channel being considered is a flat fading channel with Rayleigh distribution. Finally, it is assumed that the channel is known at the receiver. A simplified flow of signals from each transmitter end to receiver end is presented here. The presentation also includes the dimensions of the various blocks that have been used to condition the signal as it travels from one of the transmit antennas to one of the receive antennas.

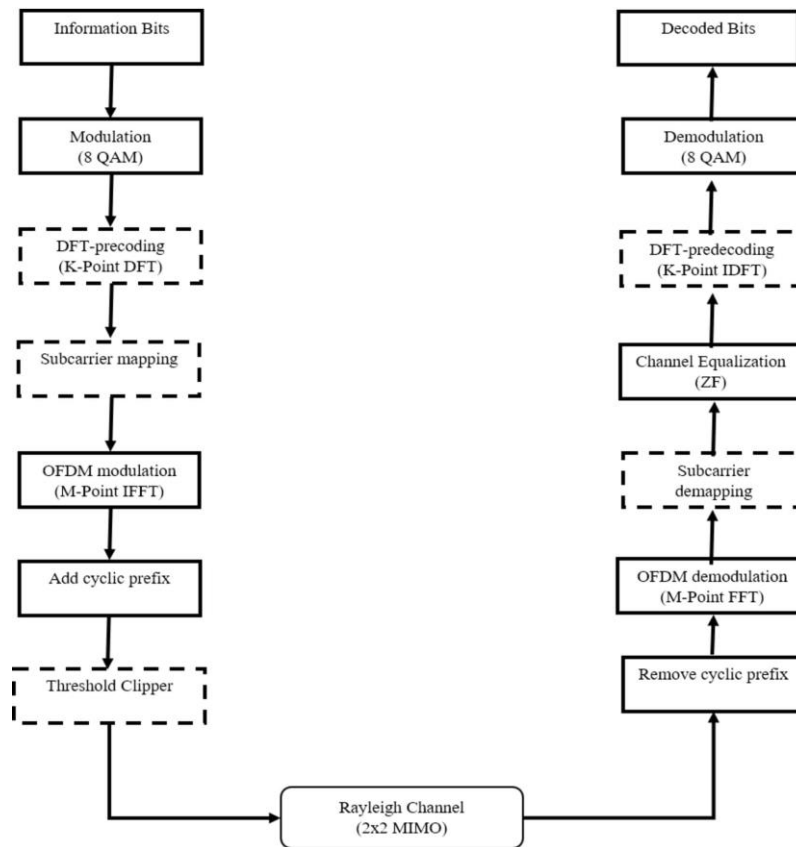


Fig. 3 Illustrative model of the implemented system

4.1. Signal Definition

We consider the discrete-time equivalents of all the signals in their complex baseband interpretations. We use upper case alphabets to denote matrices while the vectors are being denoted by lower case alphabets. The quantity of users and of the subcarriers corresponding to every signal are indicated by using superscripts and subscripts with these signals respectively. Various operators such as transpose, Hermitian and pseudo-inverse are represented by $(\cdot)^T$, $(\cdot)^H$ and $(\cdot)^\dagger$ respectively.

4.2. Transmitter Structure

Throughout the mathematical analysis, a system with Q symbols is assumed while considering the symbol index q spanning from 0 to $Q-1$. The coarse data corresponding to every symbol is characterized as $d^{(q)}$. This data is initially modulated onto the eight symbols encapsulating the 8-QAM modulation scheme. For each symbol q , the modulated symbol is represented by $s_k^{(q)}$ where K represents the number of subcarriers assigned to a specific symbol.

The modulated symbols are then translated into the frequency domain by considering their K -point FFT in a DFT-precoded system. The DFT-precoding process is represented by a square matrix with the order $K \times K$ represented by F_k . The subcarrier mapping block then maps the K DFT-precoded symbols to K among M subcarriers where $M > K$. This is done by the $M \times K$ subcarrier mapping matrix represented by $T^{(q)}$. $T^{(q)}$ can be any one among the forms presented by (1), (2) and (3) based on the subcarrier mapping technique. These two blocks are represented by dotted lines in Fig. 3 to indicate that these operations have been modified to obtain the various test case results.

$$T_{IFDMA}^{(q)}(m, k) = \begin{cases} 1, & m = kQ + q \\ 0, & \text{otherwise} \end{cases}, \quad (1)$$

$$T_{LFDMA}^{(q)}(m, k) = \begin{cases} 1, & m = qK + k \\ 0, & \text{otherwise} \end{cases}, \quad (2)$$

$$T_{B-IFDMA}^{(q)}(m, k) = \begin{cases} 1, & m = p\frac{M}{P} + l + qL \\ 0, & \text{otherwise} \end{cases}. \quad (3)$$

OFDM is then realized by taking an M -point IFFT of the signal followed by adding a cyclic prefix (CP) of an appropriate length. It is worthwhile to mention here that the CP addition as well the clipping (to induce nonlinearities) operation are not included in the mathematical representations. The reason for this being that cyclic prefix is nothing but mere addition of a few bits (and their removal on the receiver side) and has no profound impact on the system's mathematical model as long as its length is at least equal to the channel delay spread. The transmit signal in a system employing DFT-precoding is hence, mathematically represented by (4).

$$x_M^{(q)} = F_M^H \cdot T^{(q)} \cdot F_k \cdot s_k^{(q)}. \quad (4)$$

The transmit signal in a system with no DFT-precoding is similar to (4) barring the DFT-Precoding matrix F_k .

4.3. Receiver structure

This signal then passes through the Rayleigh channel with its channel coefficient matrix corresponding to the q th symbol given as $H^{(q)}$. The transmitted signal is additionally distorted by the addition of the white Gaussian noise (AWGN) represented by W_M . The received signal is mathematically represented by (5).

$$r_M^{(q)} = H^{(q)} \cdot x_M^{(q)} + W_M. \quad (5)$$

Once the signal is received at the receiver, the CP is firstly removed. This is succeeded by performing an M-point FFT to accomplish OFDM demodulation. Subcarrier demapping is then performed by using the $K \times M$ SC demapping matrix $T^{(q)\dagger}$ which represents the pseudo inverse corresponding to the SC mapping matrix $T^{(q)}$. A ZF equalizer is utilized then for rectifying the channel imperfections. The matrix of the equalizer coefficients in our mathematical modelling is denoted by a matrix $C^{(q)}$. DFT-predecoding is then employed in the cases including DFT-precoding on the transmitter side. The signal is thereafter demodulated for obtaining the estimate of the signal being transmitted. An estimate of the source signal that is being conditioned on the receiver side is mathematically given by (6).

$$\widehat{S}_k^{(q)} = F_k^H \cdot C^{(q)} \cdot T^{(q)\dagger} \cdot F_M \cdot r_M^{(q)}. \quad (6)$$

4.4. Nonlinearities Modelling

In order to analyze performance in nonlinear environments, we have introduced a simple threshold clipper model at the transmitter side. This is a simple clipper that ignores the impact of the phase distortion and considers the amplitude distortion alone, but the same analysis can be applied to more complex models among the ones found in [26] as well. The mathematical equation of the threshold clipper with an input signal $x(t)$, an output signal $x^c(t)$ and a threshold T is given by (7).

$$x^c(t) = \begin{cases} x(t), & |x(t)| \leq T \\ T e^{i \arg\{x(t)\}}, & |x(t)| > T \end{cases} \quad (7)$$

Nonlinearities in this work have been introduced by clipping off 30% of the signal input to the threshold clipper.

5. RESULTS

This section presents the results we obtained by performing various simulations. The parameters used to perform simulations are presented in Table 1. It should be noted that we have not considered IFDMA scheme while analyzing the results in the nonlinear environments. This is due to the fact that the threshold clipping model does not clip the IFDMA signal in the time domain the way that we would like, without pulse shaping. The reason for this is that the IFDMA can be visualized as a symbol being upsampled in the frequency domain. On taking its IFFT, we merely obtain the replication of the initial time domain symbols. Thus, instead of clipping the whole IFDMA symbol by some amount, the threshold clipper will rather distort each repetition of the symbol which is obviously not what we want. We would need to introduce pulse shaping in the work to be able to analyze the performance of IFDMA which has not been considered in this work.

Table 1 Simulation Parameters

Parameters	Values
Total subcarriers (M)	1024
Subcarriers/user (K)	256
Subcarriers/block (BIFDMA only)	8
Modulation	8-QAM
Equalization	ZF
Channel estimation	Perfect
Channel type	Flat fading channel
Fading channel distribution	Rayleigh distribution
Number of transmit antennas	2
Number of receiver antennas	2

5.1. Performance Evaluation of DFT-Precoding

This section presents the results indicating the effect of DFT-precoding on a MIMO-OFDM system in linear and nonlinear environments. Moreover, both the single access and multiaccess systems are considered.

5.1.1. Single access communication

Linear environment: Fig. 4 indicates the impact of DFT-precoding on a MIMO-OFDM system in linear environment. As is clear from the figure, the system with DFT-precoding indicates the best BER performance throughout. The BER for a DFT-precoded system is low because of the spreading gain caused by DFT-precoding in a MIMO-OFDM system.

Nonlinear environment: The impact of DFT-precoding on a MIMO-OFDM system in a nonlinear environment is presented in Fig. 5. It is to be noted that 30% clipping indicates that around 77 out of the 256 samples of the MIMO-OFDM signal are being distorted by the nonlinear amplifier. The results are still consistent with those found in Fig. 4 with the only difference that the BER at higher SNR is not that low as in Fig. 4 especially for non DFT-precoded system. For example, for non DFT-precoded system in Fig. 4, the BER of 10^{-1} is achieved at 17dBs while in Fig. 5, the same BER target is achieved at around 20dBs. This difference between the two figures in the case of DFT-precoded system is not that profound may be due to the lower PAPR achieved as a result of DFT-precoding. There is however, a levelling effect in BER at higher SNR values in the linear environment with DFT-precoding which is not present in the DFT-precoded case with nonlinear environment. On the other hand, when the DFT-precoded system is compared with the system with no DFT-precoding, we have higher fluctuations in envelope in non DFT-precoded systems that would ultimately result in larger out-of-band interference in nonlinear environments. The situation is further exacerbated in non DFT-precoded systems due to the lack of spreading gain that is inherent to DFT-precoded systems as mentioned before.

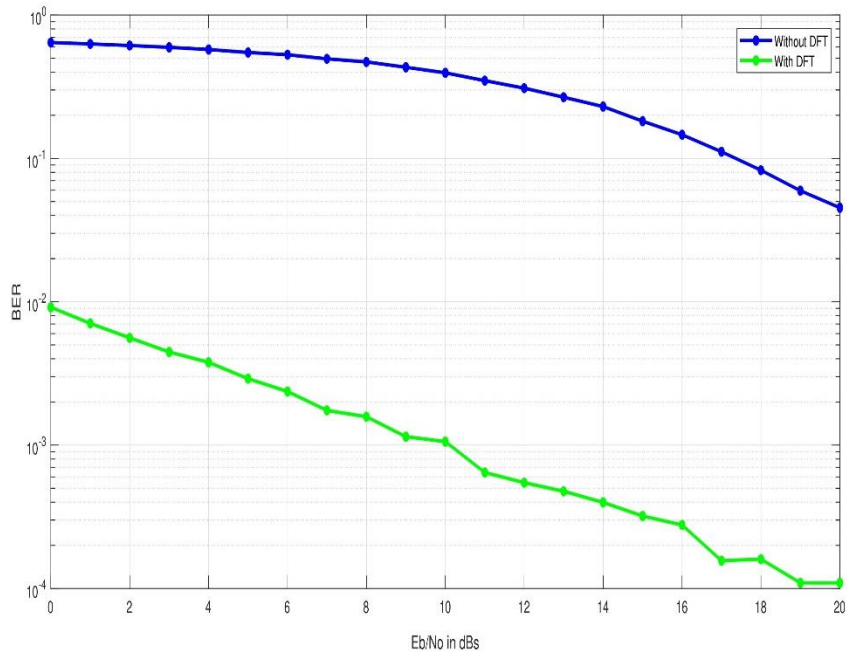


Fig. 4 Impact of DFT-precoding on MIMO-OFDM under linear conditions

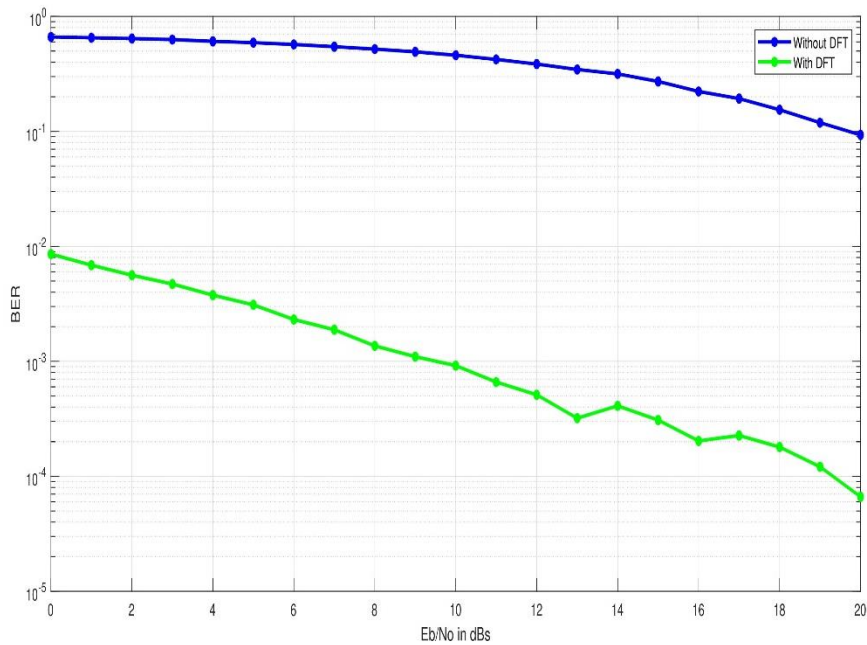


Fig. 5 Impact of DFT-precoding on MIMO-OFDM under nonlinear conditions

5.1.2. Multiaccess communication

This section presents the impact of DFT-precoding on a multiaccess MIMO scheme in linear and nonlinear environments. LFDMA is the multiaccess scheme that has been considered in this simulation. As expected, the DFT-precoding portrays higher spreading gain in the multiaccess schemes as well in both linear and nonlinear environments, as evident from the DFT-precoding schemes offering better BER performance than the non DFT-precoding schemes. Additionally, the performance in nonlinear environments is further exacerbated due to the out-of-band interference. This impact is worse in non DFT-precoded systems while in the case of DFT precoding systems, the linear and nonlinear environments offer almost identical performance at higher SNRs beyond 16dBs probably due to the ability of DFT-precoding to reduce the out-of-band interference caused by nonlinearities. These results are depicted graphically in Fig. 6.

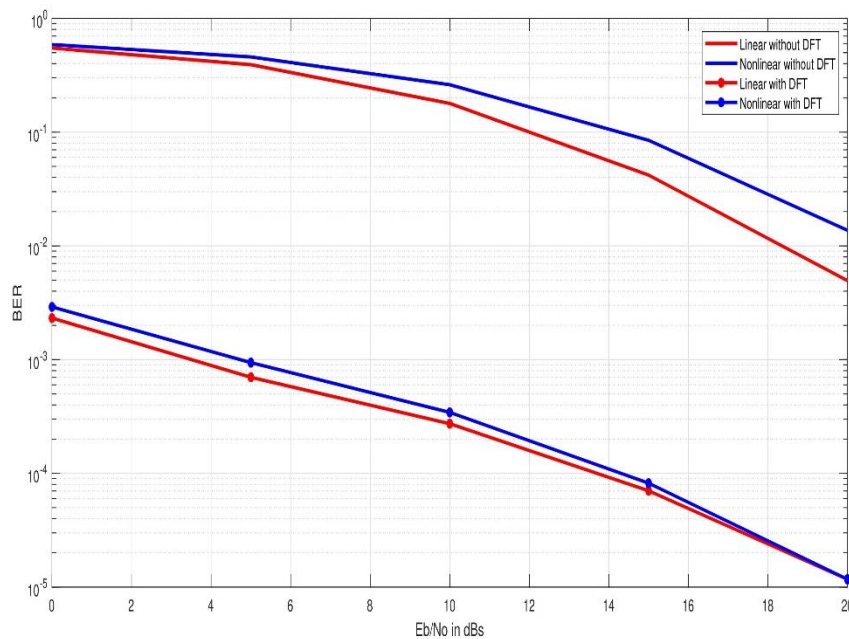


Fig. 6 DFT-precoding impact on MIMO-LFDMA under linear and nonlinear environments

5.2. Performance evaluation of subcarrier mapping schemes

This section presents the details of the analysis of a multiaccess MIMO-OFDM system employing the various subcarrier mapping schemes in linear and nonlinear environments. As discussed before, the simulations with nonlinearities do not include IFDMA.

5.2.1. Linear environment

Fig. 7 depicts the BER performance of the various MIMO-OFDMA subcarrier mapping schemes being operated in linear environment. While the performance at lower SNRs (under 10dBs) is hard to separate, the interleaved subcarrier mapping schemes (IFMDA

and BIFDMA) performance beyond 10dBs beats LFDMA quite clearly. The situation at higher SNRs in MIMO-OFDMA seems to be dominated by the spatial diversity gains offered by MIMO and hence the performance with IFDMA matches that of BIFDMA. LFDMA scheme inherently lacks the amount of diversity in comparison and this effect becomes more profound beyond 10dBs of SNR.

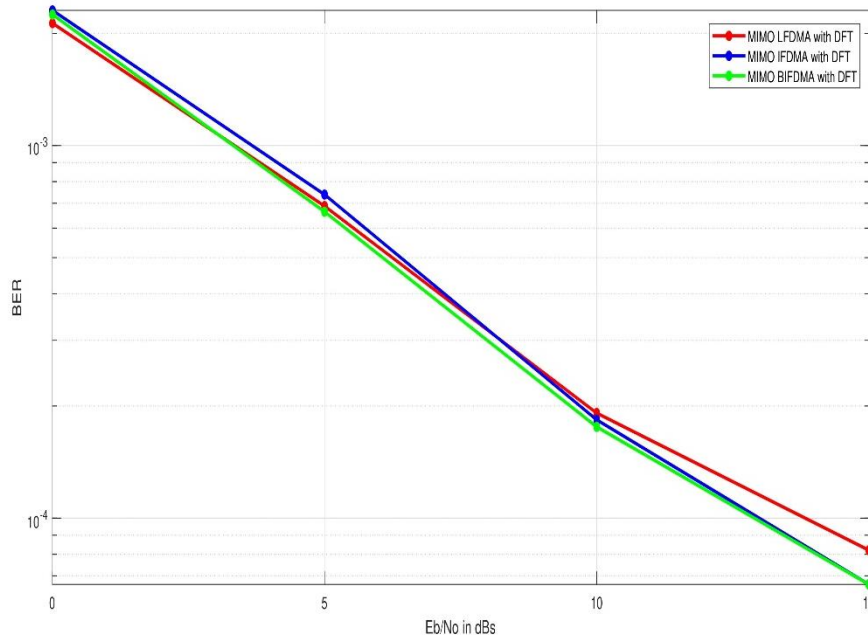


Fig. 7 BER performance analysis of various subcarrier mapping schemes under linear conditions

5.2.2. Nonlinear environment

The BER performance comparison of BIFDMA and LFDMA MIMO systems under nonlinear environments is presented here and depicted in Fig. 8. It must be noted that the SC mapping in this work maps the 256 subcarriers to 256 out of 1024 subcarriers at the output of the subcarrier mapping block. While the mapping is localized in LFDMA, it is interleaved considering a block size of 8 in BIFDMA. Clipping off 30% of the subcarrier mapped signal hence, means around 307 out of the 1024 samples would be clipped off. BIFDMA clearly beats LFDMA at SNR beyond 15dBs in terms of BER performance. The reason for this behavior is based on the envelope of the signal input to the high-power amplifier (modelled by the threshold clipper). The out-of-band leakage instigated by the nonlinear distortion of the amplifier is dependent on the input signal's envelope [27] whereby, BIFDMA consists of considerably smaller envelope fluctuations as compared to LFDMA, especially when no signal oversampling and windowing is considered [14]. Thus, the lower envelope variations characterized by BIFDMA seem to be responsible for its superior performance in terms of BER in comparison to its LFDMA counterpart as far as nonlinear environments are concerned.

5.3. Peak-to-average power ratio (PAPR) analysis

PAPR reduction techniques play an important role in allowing wireless communication technologies to abide by rigorous standards necessary for modern telecommunications including reasonable value of the BER [28]. This section presents the PAPR analysis of the multiaccess test cases where the impact of DFT-precoding has been observed. The detailed explanation of the test cases has already been presented in section 5.1.2 of the paper. It is a well-known fact that DFT-precoding has a significant effect on the PAPR of the system which in turn leads to a profound impact on the BER performance especially when amplifier nonlinearities are considered. The PAPR of the various test cases in dBs is given in Fig. 9. The difference in PAPR with and without DFT-precoding in all the test cases is clearly evident. This reduced PAPR plays a major role in the BER performance particularly in nonlinear environments, where it results in reduction of out-of-band interference that is induced by the high-power amplifier.

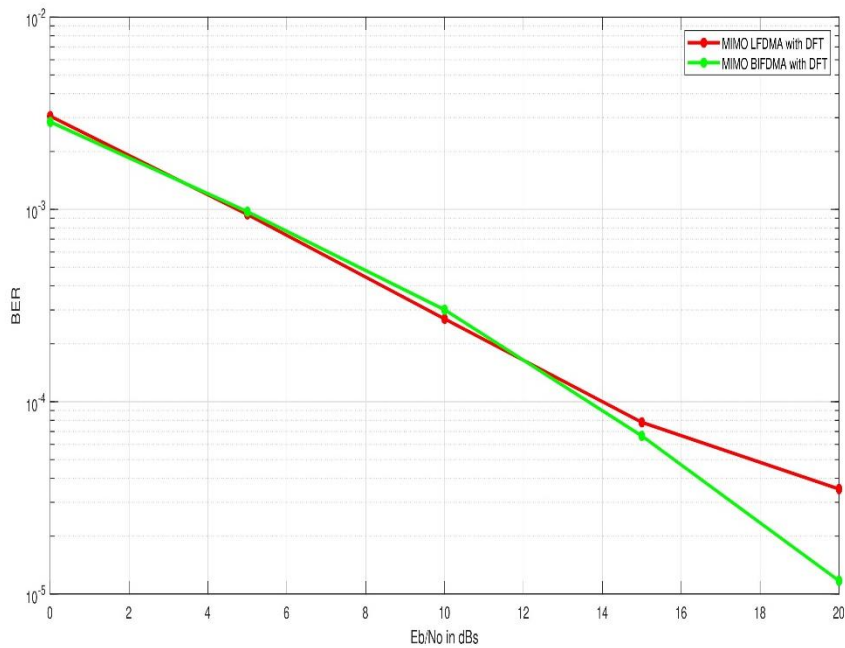


Fig. 8 LFDMA vs BIFDMA MIMO BER performance in nonlinear environments

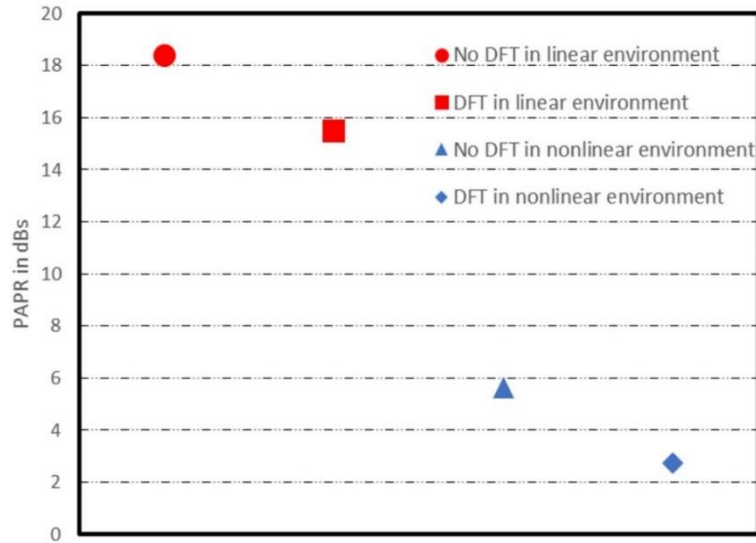


Fig. 9 PAPR analysis of Multiaccess communication in various environments

6. CONCLUSIONS

This section presents the conclusions based on the simulations performed in this research work. It was found that DFT-precoding results in reduced BER over a wide range of SNR values mainly due to its spreading gain under linear environments. This trend is complemented further by its reduced PAPR thereby resulting in reduced impact of HPA nonlinearities in nonlinear environments. Comparing DFT-precoded systems in linear and nonlinear environments resulted in almost identical performance at higher SNRs. This was probably due to the envelope fluctuations taken out of the equation by DFT-precoding while the spreading gain is the same in both the cases. For the subcarrier mapping schemes, it was observed that the interleaved mapping schemes outperformed the non-interleaved schemes comprehensively under both linear and nonlinear environments. This was due to their greater spreading gain complemented by their reduced envelope fluctuations under nonlinear environments. The BER results were further validated by simulating and examining the PAPR reduction in schemes with DFT-precoding under various environments.

Pulse shaping was not considered in this work which limited our tests in nonlinear multiaccess environments to BIFDMA and LFDMA only. The future directions of this work may be to include pulse shaping to make the results more holistic. Furthermore, we can also consider a diverse range of more channel environments among the ones found in [29] to perform more realistic analysis of the considered test cases. Finally, the results can be refined further by considering other nonlinearity models among the ones found in [30] that consider amplitude as well as phase distortion.

REFERENCES

- [1] L. Zhang, A. Ijaz, P. Xiao, M. M. Molu and R. Tafazolli, "Filtered OFDM systems, algorithms, and performance analysis for 5G and beyond", *IEEE Trans. Commun.*, vol. 66, no. 3, pp. 1205–1218, March 2018.
- [2] R. C. Kizilirmak and H. K. Bizaki, "Non-orthogonal multiple access (NOMA) for 5G networks", in *Towards 5G Wireless Networks-A Physical Layer Perspective*, Intech Open, 2016, pp. 83–98.
- [3] S. Dhua, R. Arjun, K. Appaiah and V. M. Gadre, "Low complexity FBMC with filtered ofdm for 5G wireless systems", In Proceedings of the IEEE International Conference on Signal Processing and Communications (SPCOM), 2020, pp. 1–5.
- [4] C. He, L. Zhang, J. Mao, A. Cao, P. Xiao and M. A. Imran, "Performance analysis and optimization of DCT-based multicarrier system on frequency-selective fading channels", *IEEE Access*, vol. 6, pp. 13075–13089, 2018.
- [5] R. Qomarrullah, I. W. Mustika and S. Dharmanto, "Performance comparison of SISO and MIMO-OFDM based on SDR platform", In Proceedings of the 3rd International IEEE Conference on Science and Technology-Computer (ICST), 2017, pp. 142–146.
- [6] A. Ahrens, and C. Benavente-Peces, "Modulation-mode and power assignment in broadband MIMO systems", *Facta Univ.: Electron. Energ.*, vol. 22, no. 3, pp. 313–327, Dec. 2009.
- [7] E. Björnson, J. Hoydis and L. Sanguinetti, "Massive MIMO has unlimited capacity", *IEEE Trans. Wirel. Commun.*, vol. 17, no. 1, pp. 574–590, Jan. 2018.
- [8] M. N. Seyman and N. Taşpinar, "Symbol detection using the differential evolution algorithm in MIMO-OFDM systems", *Turk. J. Electr. Eng. Comput. Sci.*, vol. 21, no. 2, pp.373–380, March 2013.
- [9] Y. Medjahdi, S. Traverso, R. Gerzaguët, H. Shaiek, R. Zayani, D. Demmer, R. Zakaria, J.-B. Doré, M. B. Mabrouk and D. Le Ruyet, "On the road to 5G: Comparative study of physical layer in MTC context", *IEEE Access*, vol. 5, pp. 26556–26581, 2017.
- [10] K. S. Ali, H. ElSawy and M.-S. Alouini, "On mode selection and power control for uplink D2D communication in cellular networks", In Proceedings of the IEEE International Conference on Communication Workshop (ICCW), 2015, pp. 620–626.
- [11] J. Zhang, L.-L. Yang, L. Hanzo and H. Gharavi, "Advances in cooperative single-carrier FDMA communications: Beyond LTE-advanced", *IEEE Commun. Surv. Tutor.*, vol. 17, no. 2, pp. 730–756, 2015.
- [12] N. Taşpinar and Ş. Şimşir, "An efficient technique based on firefly algorithm for pilot design process in OFDM-IDMA systems", *Turk. J. Electr. Eng. Comput. Sci.*, vol. 26, no. 2, pp. 817–829, March 2018.
- [13] Y. Zhang, A. Ghazal, C.-X. Wang, H. Zhou, W. Duan and E.-H. M. Aggoune, "Accuracy-complexity tradeoff analysis and complexity reduction methods for non-stationary IMT-A MIMO channel models", *IEEE Access*, vol. 7, pp. 178047–178062, 2019.
- [14] H. Ochiai, "Statistical distributions of instantaneous power and peak-to-average power ratio for single-carrier FDMA systems", *Phys. Commun.*, vol. 8, pp. 47–55, Sept. 2013.
- [15] A. Elsanousi and S. Oztürk, "Performance analysis of OFDM and OFDM-MIMO systems under fading channels", *Eng. Technol. Appl. Sci. Res.*, vol. 8, no. 4, pp. 3249–3254, Aug. 2018.
- [16] A. Agarwal and S. N. Mehta, "Performance analysis and design of MIMO-OFDM system using concatenated forward error correction codes", *J. Cent. South Univ.*, vol. 24, no. 6, pp. 1322–1343, July 2017.
- [17] A. H. Alqahtani, K. Humadi, A. I. Sulyman and A. Alsanie, "Experimental Evaluation of MIMO-OFDM System with Rateless Space-Time Block Code", *Hindawi Int. J. Antennas and Propag.*, p. 6804582, Feb. 2019.
- [18] S. Kinjo, "A. Tomlinson-Harashima, Precoding for DFT-spread MIMO-OFDM systems", *IEICE Commun. Express*, vol. 1, no. 4, pp. 148–153, Sept. 2012.
- [19] J. Tao, "DFT-precoded MIMO OFDM underwater acoustic communications", *IEEE J. Ocean. Eng.*, vol. 43, no. 3, pp. 805–819, July 2018.
- [20] J. Tao, L. An, S. Yao, L. Zhou, X. Han and Z. Qin, "Precoded OFDM over underwater acoustic channels", In Proceedings of the Thirteenth ACM International Conference on Underwater Networks & Systems, 2018, pp. 1–6.
- [21] H. A. Mohamad, A. Idris and K. Dimiyati, "MIMO-OFDMA subcarrier mapping improvement by using quarter ICI-SC with STFBC technique", *J. Telecommun. Electron. Comput. Eng. (JTEC)*, vol. 9, no. 1–4, pp. 33–36, 2017.
- [22] M. Rakshit, S. Bhattacharjee, J. Sanyal and A. Chakrabarti, "Hybrid turbo coding pts with enhanced switching algorithm employing de to carry out reduction in papr in aul-based MIMO-OFDM", *Arab. J. Sci. Eng.*, vol. 45, no. 3, pp. 1821–1839, March 2020.
- [23] M. Rakshit, S. Bhattacharjee, G. Garai and A. Chakrabarti, "A Novel Distributive Population-Based Differential Evolution Algorithm for SLM Scheme to Reduce PAPR in Massive MIMO-OFDM Systems", *SN Comput. Sci.*, vol. 1, no. 5, pp.1–17, Sept. 2020.

- [24] D. Tse and P. Viswanath, *Fundamentals of wireless communication*. Cambridge university press, 2005.
- [25] K. Sankar, "MIMO with ML equalization", *E-notes on www.dsplog.com*, posted on December 14 2008.
- [26] K. M. Gharaibeh, *Nonlinear distortion in wireless systems: Modeling and simulation with MATLAB*, John Wiley & Sons, 2011.
- [27] T. Frank, "Block-interleaved frequency division multiple access and its application in the uplink of future mobile radio systems", *Ph.D. dissertation*, Technische Universität Darmstadt, 2010.
- [28] B. D. Jovanović and S. Milenković, "The peak windowing for PAPR reduction in software defined radio base stations", *Facta Univ.: Electron. Energ.*, vol. 33, no. 2, pp. 273–287, June 2020.
- [29] J. Meinilä, P. Kyösti, T. Jämsä and L. Hentilä, "Winner II channel models", in *Radio Technologies and Concepts for IMT-Advanced*, pp. 39–92, Oct. 2009.
- [30] M. C. P. Paredes, F. Grijalva, J. Carvajal-Rodríguez and F. Sarzosa, "Performance analysis of the effects caused by HPA models on an OFDM signal with high PAPR", In *Proceedings of the IEEE Second Ecuador Technical Chapters Meeting (ETCM)*, 2017, pp. 1–5.